2010

ARTERIAL WAVEFORM MEASUREMENT USING A PIEZOELECTRIC SENSOR

Ruizhi Zhang
Virginia Commonwealth University

Department of Biomedical Engineering
Virginia Commonwealth University

This is to certify that the thesis prepared by Ruizhi Zhang entitled ARTERIAL WAVEFORM MEASUREMENT USING A PIEZOELECTRIC SENSOR has been approved by his committee as satisfactory completion of the thesis requirement for the degree of Master of Science in Biomedical Engineering.

Paul A. Wetzel, Ph.D., Associate Professor, School of Engineering

Kevin R. Ward, MD., Professor, School of Medicine

Ding-Yu Fei, Ph.D., Associate Professor, School of Engineering

Gerald E. Miller, Ph.D., Chair, Biomedical Engineering, School of Engineering

Rosalyn Hobson, Ph.D., Assistant Dean of Graduate Affairs, School of Engineering

Russell D. Jamison, Ph.D., Dean, School of Engineering

F. Douglas Boudinot, Ph.D., Dean, school of Graduate Studies

August 9, 2010

Date

ARTERIAL WAVEFORM MEASUREMENT USING A PIEZOELECTRIC SENSOR

A thesis submitted in partial fulfillment of the requirements for the degree of Master of Science at Virginia Commonwealth University

by

RUIZHI ZHANG
B.S., Huazhong University of Science and Technology, China, 2007

Director: PAUL A. WETZEL, Ph.D.
Associate Professor, Department of Biomedical Engineering

Virginia Commonwealth University
Richmond, Virginia
August, 2010

Acknowledgments

First, I would like to express my sincere gratitude to my advisor Dr. Paul A. Wetzel for the great help and guidance he provided throughout my research. I would also like to thank Dr. Kevin Ward for his insightful suggestions for my thesis and Dr. Ding-Yu Fei as my thesis committee member.

I would like to convey my appreciation to my colleagues Richie Boe and Stacey Houston for their help in the project. I also want to thank my lab mates, class mates, and faculty and staff in the Department of Biomedical Engineering. They made my graduate study a great journey of life.

I would like to thank my parents for their unconditional love and support all the time. And I thank all of my friends for their company and encouragement.

The author also wishes to acknowledge the partial support received form Progeny Systems, Grant Number PSC-0117, K. R. Ward, (PI) and P.A. Wetzel (co-PI) titled: Smart Physiological Monitor for the Critical Care Transport Team.

Table of Contents

List of Abbreviations

AIx	Augmentation Index
ECG	Electrocardiography
FFT	Fast Fourier Transform
HRV	Heart Rate Variability
ICU	Intensive-care Unit
LVDT	Linear Variable Differential Transformer
NTC	Negative Temperature Coefficient
PPG	Photoplethysmography
PVDF	Polyvinylidene Fluoride
PZT	Piezoelectric Transducer
RMD	Relative Mean Difference
SpO2	Pulse Oximeter Oxygen Saturation
VM	Valsalva Maneuver
WEP	Wideband External Pulse

List of Figures

List of Tables

Abstract

ARTERIAL WAVEFORM MEASUREMENT USING A PIEZOELECTRIC SENSOR

By Ruizhi Zhang, B.S.

A thesis submitted in partial fulfillment of the requirements for the degree of Master of Science at Virginia Commonwealth University

Virginia Commonwealth University, 2010

Director: Paul A. Wetzel, Ph.D.
Associate Professor, Department of Biomedical Engineering

This study aims to develop a new method to monitor peripheral arterial pulse using a PVDF piezoelectric sensor. After comparing different locations of sensor placement, a specific sensor wrap for the finger was developed. Its composition, size, and location make it inexpensive and very convenient to use. In order to monitor the effectiveness of the sensor at producing a reliable pulse waveform, a monitoring system, including the PZT sensor, ECG, pulse-oximeter, respiratory sensor, and accelerometer was setup.

Signal analysis from the system helped discover that the PZT waveform is relative to the 1st derivative of the artery pressure wave. Also, the system helped discover that the first, second, and third peaks in PZT waveform represent the pulse peak, inflection point, and dicrotic notch respectively. The relationship between PZT wave and respiration was also analyzed, and, consequently, an algorithm to derive respiratory rate directly from the PZT waveform was developed. This algorithm gave a 96% estimating accuracy. Another feature of the sensor is that by analyzing the relationship between pulse peak amplitude and blood pressure change, temporal artery blood pressure can be predicted during Valsalva maneuver.

PZT pulse wave monitoring offers a new type of pulse waveform which is not yet fully understood. Future studies will lead to a more broadly applied use of PZT sensors in cardiac monitoring applications.

CHAPTER 1

Introduction

1.1 Historical Background

From antiquity, arterial pulse has been one of the most fundamental measures in medicinal practice. Many cultures developed qualitative interpretations of changes in the texture and strength of the arterial pulse associated with a patient's health status [1]. In traditional Chinese clinical medicine, palpation has been used as one of the four basic diagnostic methods for thousands of years. The graphic method of recording arterial pulse, however, was not discovered until 19th century. The sphygmography developed by Dr Frederick Akbar Mahomed provided a quantitative illustration of the effects of medication on the arterial pulse; it also provided a picture of the arterial waveform in hypertension and other diseases. Furthermore, these were the first ever signals that displayed time-related changes in a physiological parameter, which could then be recorded and compared with signals at different times or in different subjects [2]. By the beginning of the 20th century, sphygmography was well established in medical practice, as reported in medical journals and textbooks (Figure 1), and its ability to describe the effects of aging on arterial degeneration was widely used by life insurance companies for estimation of risk [2,3]. Unfortunately,

sphygmography lapsed with the development of the brachial cuff and the auscultatory technique to produce the sphygmomanometer in the early 20th century. This provided pressure measurements in terms of the height of a column of mercury, where values of pressure were associated with the peak (systolic pressure) and trough (diastolic pressure) of the arterial pressure pulse.

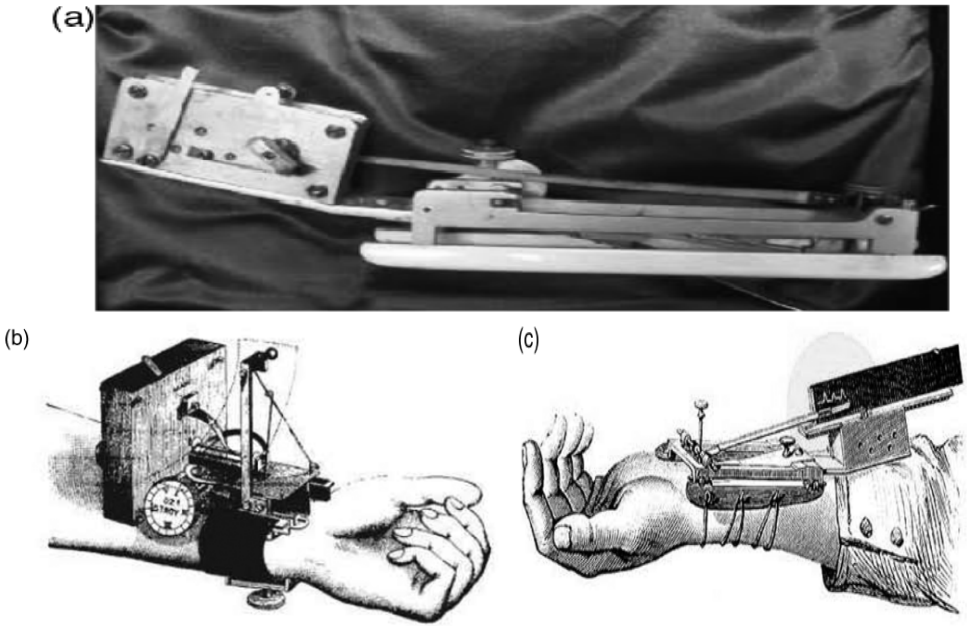

Figure 1, Sphygmography in 1800s

The figures depict the evolution of sphygmography technology in the late 1800s to the early 1900s, before the advent of the modern sphygmomanometer. (a) Sphygmomanometry instrument developed by Dr Mahomed in 1872 (Courtesy: University of Manchester Medical School Museum, 2008); (b) Sphygmomanometry device developed by Dr Dudgeon and used by Sir James MacKenzie in 1902 (Courtesy: Home´opathe International, 2001); and (c) Sphygmograph with arterial waveform recorded by a pen-recorder developed by Dr Marley in 1914 (Courtesy: Letzte A¨ nderung: June 21, 2007 [3].

The conventional sphygmomanometric measurement of brachial cuff systolic and diastolic has been widely used to quantify arterial blood pressure associated with cardiovascular risks, as well as complications with many other diseases, such as diabetes. However, it fails to provide the continuous information of arterial pressure, which is highly related to the physical properties of the elastic arteries, arterial stiffness, pulse wave velocity and

altered wave reflection as independent risk factors for cardiovascular disease. Mahomed in 1874 was also the first person to recognize the difference between pressure waves in central and peripheral arteries, while MacDonald's publication on blood flow in arteries and arterial mechanics explained this phenomenon on the basis of wave reflection and introduced transfer functions to characterize properties of vascular beds in the frequency domain [4]. Since then, the advent of the microcomputer has allowed the discovery of non-invasive techniques for accurate pulse wave recording, which led the development of pulse wave analysis.

1.2 Measurement Methods for Arterial Pressure and Pulse Wave

1.2.1 Sphygmomanometer

In 1896 Riva-Rocii invented the palpation method to measure systolic pressure with a brachial cuff inflated to obliterate peripheral pulse. With this technique, the cuff is gradually deflated until the peripheral pulse is again felt at the radial artery [5]. The cuff pressure at which the pulse is initially felt is the systolic pressure. The information required for estimation of diastolic pressure became available with Korotkoff's observation that sounds heard through the stethoscope placed over the brachial artery change [6]. As the pressure in the cuff falls, a "whooshing" or pounding sound, called the Korotkoff sound is heard when blood flow first starts again in the artery. The pressure at which this sound began is noted and recorded as the systolic blood pressure. The cuff pressure is further released until the sound can no longer be heard. This is recorded as the diastolic blood pressure [7]. A more formal description of the phase of the Korotkoff sounds was employed by Gedees, O'Brein and Fitzgerald, who divided the spectrum of the Korotkoff

sound into five different phases [8, 9]. These phases occur sequentially during the cuff deflation and Phase I, IV and V are considered useful to estimate systolic and diastolic pressure.

1.2.2 Applanation Tonometry

Since the technique of Applanation Tonometry was employed by Pressman and Newgard to measure arterial pressure wave shapes in 1963, it has become one of the most widely used type of transducer for accurate, non-invasive detection of the peripheral arterial pressure wave [10, 11]. Applying applanation tonometry (see Figure 2) involves flattening a curved surface, such that any wall tension is effectively reduced to zero and there is transmission of all internal force to the external transducer [3,12]. In this case for pulse wave acquisition, when the artery underlying the skin surface is flattened using gentle pressure of the manometer, circumferential pressures within that point of the artery are equalized and an accurate pressure waveform can be recorded (Figure 2) [3]. Because this requires a rigid support for the artery, the most accessible and suitable anatomic location is the wrist, where the radial pulse can be readily palpated. The major sensor types are the single sensor and an array of sensors. The single sensor is a piezoresistive transducer with dimensions much smaller than the arterial diameter at the end of a hand-held pencil-like stem. The array of sensors contains sensors positioned over the radial artery where the optimum signal is selected by computer algorithms [13, 14]. Accurate quantitative tonometry cannot be achieved in practice because of the soft tissue which lies between the skin and anterior wall of the artery, but measurements can be approximated by a calibration process. Accurate quantitative tonometry also

requires finding the artery correctly and maintaining a constant pressure. Therefore, there is no reliable and reproducible tonometric technique able to quantify the intra-arterial pressure in a way that matches the sphygmomanometer while maintaining an ease of long term use. However, it is highly effective in recording the time-related change in the intra-arterial pressure.

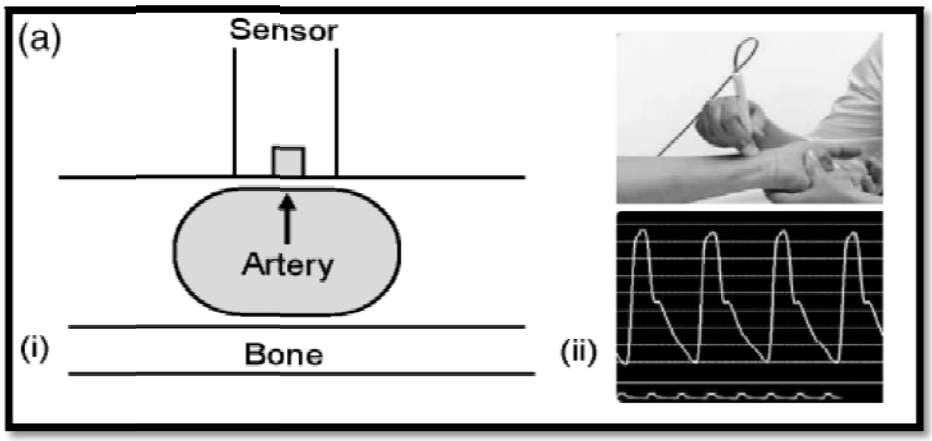

Figure 2, Applanation Tonometer

(i) Diagrammatic representation of the artery being ‘‘applanated’’ between the ultrasound sensor and the underlying hard structure—in this case, a bone. (ii) SphygmoCor Cardiovascular Management System (AtCor Medical, Sydney, Australia), one applanation tonometer and the pulse wave it recorded [3].

1.2.3 Photoplethysmography

A common method for pulse wave recording is monitoring the blood volume of the finger through Photoplethysmography (PPG). PPG is often obtained by using a pulse oximeter which illuminates the skin and measures changes in light absorption. The availability of low-cost components and microprocessor technology result in PPG being used in various commercial devices to measure parameters including blood oxygen levels, transit time, cardiac output, and beat-to-beat changes in arterial pressure. Because blood flow to the skin can be modulated by a number of other physiological systems, PPG

can also be used to monitor breathing, hypovolemia, anesthesia and other circulatory conditions. Other studies also extend the use of the PPG waveform to the detection of ventricular ejection times and pulse wave analysis, as well as the quantification of vascular function [15, 16]. Allen has provided an extensive review of PPG and its applications in physiological measurement and clinical use [17].

1.2.4 Direct Blood Pressure Monitoring

Since 1733 when Stephen Hales first attached a vertical tube to an artery of a horse and measured mean arterial pressure, the intra-arterial method has been one of the most accurate ways to measure arterial blood pressure (BP). Even today, it is widely used in critical care, operating rooms, and in these patients with low cardiac output states when pulses may be poorly palpable and Korotkoff sounds may be difficult to hear [18]. Invasive monitoring provides a moment-to-moment picture and visual display of BP trends. During direct BP monitoring, an artery is cannulated with a catheter, which is connected to fluid-filled tubing and an electronic pressure transducer system. Despite its accuracy, invasive vascular pressure monitoring can result in complications such as thrombosis, infection, air embolism, bleeding, arteriovenous fistulas, and pain [19]. Therefore, it is used mostly in patients with severe conditions and as a standard reference when compared to other non-invasive BP monitoring methods in scientific studies.

1.3 The Basis of Pulse Wave Analysis

1.3.1 Pulse Wave Features

The technique of non-invasive aortic pulse wave analysis, as used in most commercial cardiac monitoring systems, depends on three parameters:

accurate recording of the peripheral pressure wave, its calibration against brachial pressure, and generation of the ascending aortic pressure waveform through the use of a generalized transfer function in a computerized process [4]. As mentioned, understanding the different features of pulse waveform between aorta and peripheral arteries is essential. The contour of the pulse waveform at the aortic artery is determined by the pattern of ventricular ejection and the elastic and geometric properties of the arterial tree [20]. In the ascending aorta (Figure 3, left), the first inflection generally coincides with the time of peak flow velocity (at pressure value of P_i), at approximately 30% of the ejection duration [1, 21]. Systolic pressure (P_s) occurs after peak flow. The ratio of the augmented component of pressure described as $(P_s\text{-}P_i)/(P_s\text{-}P_d)$ is defined as the augmentation index (AIx). Aix has been found to have a significant heritability factor and shows changes with respect to age [1,22, 23, 24].

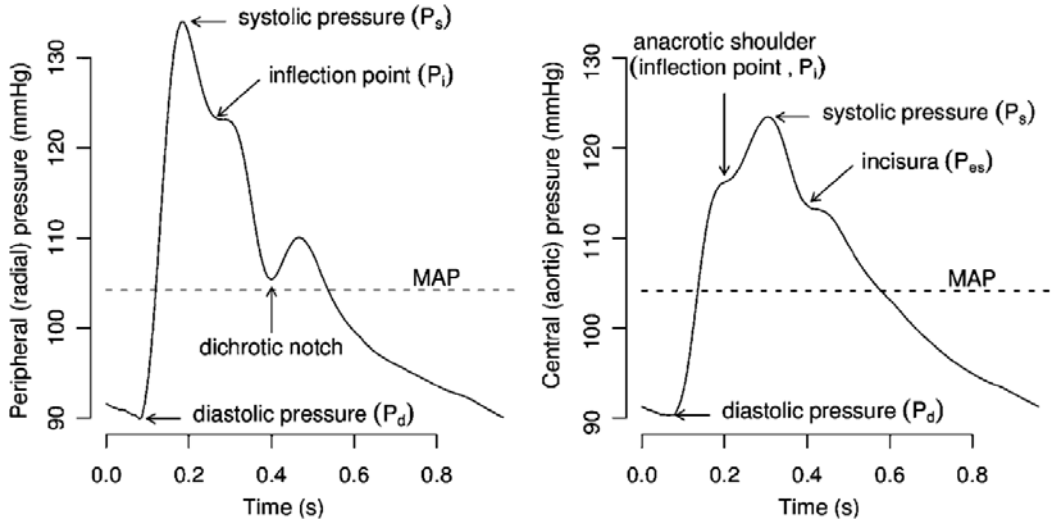

Figure 3, Peripheral and Central Pressure Waveform

Features of the radial pulse wave and corresponding central aortic pressure wave. Radial pressure wave was recorded from a 50 year old male, BMI of 23.72 kg m−2, and central pressure wave derived using an aortic-radial transfer function. MAP: mean pressure [1].

The radial pulse is also characterized by a number of waveform features (Figure 3). The minimum point in the pressure waveform corresponding to diastolic pressure (P_d) is often equated to that in the aorta and together with mean pressure is used as a calibration reference [1, 25, 26]. The first peak in the waveform corresponds to systolic pressure (P_s) and is different than the first peak of central pulse, with a large variation in the difference. An inflection (P_i) occurs late in systole and is usually lower than P_s but may form a local maximum higher than P_s in cases of high arterial stiffness, as seen with advancing age [1, 27]. A local minimum near the end of systole, labeled as the dichrotic notch, strongly correlates with the timing of the incisura obtained from the aortic pressure pulse, and therefore corresponds to aortic valve closure, and can be used to obtain systolic duration.

1.3.2 Transfer Function

Transfer functions are mathematical representations used to describe the relationship between central and peripheral pressure. The intention of this transfer function is to determine the central aortic pressure by means of peripheral arterial pressure pulse wave shape, using sphygmomanometric cuff measurements as calibration. A significant characteristic of the pressure pulse is that it changes shape as it travels away from the heart. In large arteries, mean pressure is essentially constant. Hence, shape changes are such that the total waveform area over on one cardiac period is constant, and this generally results in a change of pulse height [1]. These features were documented by Kroeker and Wood in 1955 [28] using intra-arterial catheters to record the pulse wave. After that, a simple tube model showing the change in arterial pulse and pulse amplitude amplification due to elastic and

geometric non-uniformity were studied by many researchers [1, 29, 30, 31, 32]. The study by Karamanoglu in 1993 formed the basis for the development of a generalized transfer function, where it was proposed that the transfer function could be applied to adults for the non-invasive estimation of central aortic pressure [1, 33]. There have been other attempts at individualization and development of group-specific functions [1, 34, 35] showing that individual differences should be considered when applying a transfer function.

1.4 Objective of This Study

It is assumed that the pulse waveform signal contains much more information than just systolic and diastolic blood pressure, and current major monitoring methods such as applanation tonometry, photoplethysmography, and intra-arterial measure all have deficiencies at some level. The objective of this study is to develop a new pulse wave monitoring system using a PVDF piezoelectric sensor and to compare the features of the obtained wave form to that of a PPG. A further objective of this study is to find any correlation between pulse waves and respiration using pulse wave analysis. Different types of maneuvers are also monitored to determine waveform changes that may correspond to physiological conditions.

CHAPTER 2

Material and Device Construction

2.1 Piezoelectric PVDF Sensor

Creating an acceptable sensor to monitor blood pressure is one of the most important components of this study. An acceptable sensor is one that is sensitive, reliable, non-toxic, and inexpensive. Of these factors, sensitivity is of major concern given that the sensor must detect subtle changes through the skin caused by the pulsation of the artery. While sensitivity is of vast importance, the signal from the sensor also needs to be in a voltage large enough to allow the user to differentiate between noise and the actual measurement.

PVDF is a highly non-reactive and purely thermoplastic fluoropolymer. The strong piezoelectricity of a PVDF was observed by Kawai in 1969 [36]. The piezoelectric coefficient of the polarized thin films were reported to be as large as 6-7 pC/N, which is 10 times larger than that observed in any other polymer [37]. As pressure is applied to the PVDF sensor, the film of the sensor flexes to generate an electric potential which is amplified, then acquired through a data acquisition system and recorded by computer for later analysis. The sensor is sensitive to mechanical strain which means it can monitor the change of applied pressure but does not respond to a sustained or

unchanged pressure. In this study, expansion of the blood vessel as blood passes through the artery is captured by the sensor and then transformed into an electrical signal. The electrical signal is displayed on the computer screen and labeled as the piezoelectric transducer (PZT) pulse waveform. The PZT pulse waveform is not like the traditional pulse waveform which represents actual blood pressure over time. Instead, it represents the change in blood pressure over time.

A commercially available piezoelectric adult snore sensor manufactured by Dymedix Corporation (Shoreview, Minnesota) was initially used to evaluate potential recording measurement locations throughout the body. At first, the sensor was placed on radial, brachial and temporal arteries separately to test the quality of signal waveform. One of the problems is that the sensor required sustained pressure to maintain close contact with the arteries through the skin and soft tissue. Manually pressing the sensor at the correct spot often resulted in a better signal waveform. It was found however, the human hand cannot maintain a stable pressure in a long term setting which creates a greater opportunity for false readings. A stretch band was then used to try to prevent this problem, since the band stretch pressure is evenly dispersed and constant. Signal strength, however, is not as good as manually pressing the sensor to the test location. Even though, pulse waves captured on these spots were very helpful in initially observing this new type of pulse waveform, in order to do more extensive things such as discover the correlation between PZT pulse waves and respiration and predict head blood pressure, a more reliable sensor needed to be created.

Considering that one of the major tasks of this project was to develop a

method for long term monitoring of pulse wave, both a head band and arm band were rendered uncomfortable and inconvenient. A much smaller sensor on the finger seemed to be more suitable for this purpose. Unfortunately, the adult snore sensor made by Dymedix Corporation could not be used to accomplish this task since the padding was too stiff to curve and conform to the curvature of the finger. Thus a more flexible sensor had to be developed.

Using the parts and materials provided by Dymedix Corporation, a new sensor, more suitable for testing pulse from finger, was designed. The materials include a roll of PVDF film, two conductor lead wire with oval tabs, and a sheet of ARclad. ARclad is high-performance industrial pressure-sensitive adhesive with good electrical conductivity. The PVDF film is like a dual plate capacitor, so it had to be precisely with a very sharp pair of scissors to avoid shorting out the two sides of the film. The sensitivity of PVDF film to stress and or stretching is different along two directions. Cutting the film along the poling direction provides 7 times better sensitivity in contrast to the other direction (Dymedix documentation). A rectangle shape film was cut to a length of 5cm and width of 1cm. The length of the longer side is about one-half to two-thirds of the girth of the base segment of the finger. Therefore the film could fully cover the artery area alongside the finger bone while still not overlapping. Then, the supplied wire was affixed, using a small amount of ARclad placed between the wire tab and the center of the short edge of the metalized PVDF film sensor surface, on both sides. To avoid shorting out the sensor, extreme care was exercised when preparing the custom made sensors, particularly when applying the ARclad conductive adhesive paste for attaching the electrodes to each side of the film. The entire sensor assembly

was then carefully covered with surgical tape to avoid direct contact between the sensor film and the skin.

(1) (2)

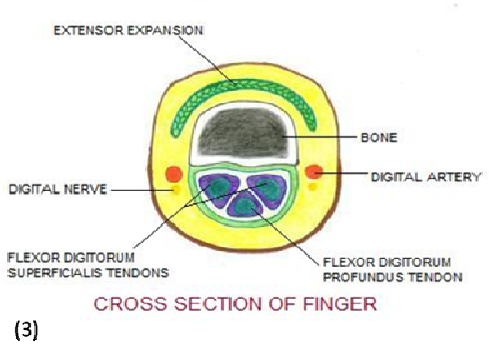

(3)

Figure 4, Piezoelectric Sensor on Finger

(1) Piezoelectric sensor sticking to stretching band with two foam padding; (2) Sensor wrapped on index finger; (3) Cross section of finger downloaded from http://www.joint-pain-expert.net/finger-anatomy.html

As Figure 4 (1) shows, a sensor was attached to a stretching band with elasticity to provide pressure and maintain close contact between sensor and finger. The signal source was two digital arteries located on both sides of the finger slightly lower than proximal phalange as Figure 4 (3) shows. To enhance the contact between the sensor and digital arteries, two foam pads were added under the sensor surface to push the sensor to the skin right on top of the arteries.

The signal form the newly configured finger sensor was remarkably improved in comparison to the signal from the pre-constructed sensor by

Dymedix. Most importantly, attaching the sensor to the finger only takes seconds; it is much easier and faster than testing at the wrist, elbow, or temple and avoids lengthily time searching for the correct arterial location. As a result the majority of tested was performed with the custom sensor from the location of the finger.

2.2 Circuit Construction

As Figure 5 shows, an instrumentation Amplifier model AD524 (Analog Devices, Norwood, MA) was used as the differential amplifier in the circuit. The gain of the amplifier was set to 10 which provided an output signal with a range of 1 to 10 volts. A passive low-pass filter with a cutoff frequency at 20 Hz was used after signal amplifying to remove any 60 Hz noise. A 16 bit resolution multichannel Biopac MP150 data acquisition system (BioPAC, Los Gatos, CA) was used as the analog-to-digital converter with a sampling rate of 200 Hz. The input range of the Biopac MP150 system was ±10V. After amplifying and filtering, the analog signal was converted to a digital signal by Biopac then the signal was recorded and displayed on the computer.

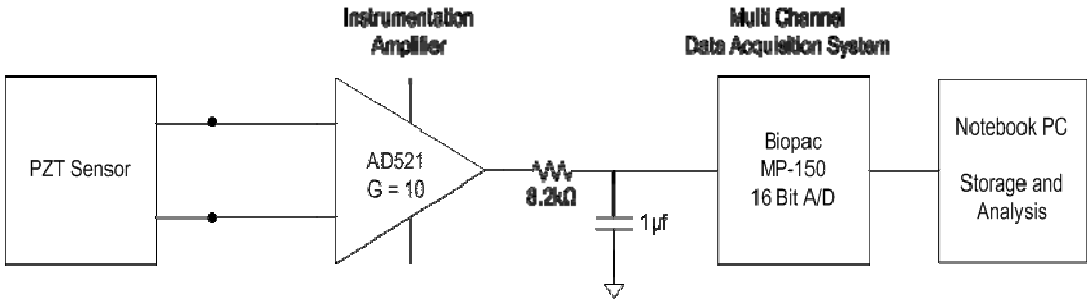

Figure 5, Circuit Diagram of PZT Pulse Wave Monitor

2.3 Monitoring System with Other Physiological Measurements

To fully understand the PZT pulse waveform, comparisons with other existing methods of cardiovascular monitoring were required. Based on the present lab equipment, a 3-lead electrocardiography (ECG) equipment (Criticare Systems, Walkasaukee, WI), and a pulse-oximeter were used during the tests as references. The analog output of the ECG signal and photoplethysmography were connected to the Biopac as well as the PZT signal, so that a comparison of the three waveforms could be recorded simultaneously during each test. To measure breathing, a negative temperature coefficient (NTC) type thermistor was used as a respiratory monitor to record the respiration information which is relative to cardiovascular system conditions [38]. An accelerometer was also placed on the same finger as the piezoelectric sensor to record the movement of the testing spot as a method to distinguish and/or eliminate the PZT pulse waveform noise caused by unwanted movement of the body. Thus a monitoring system based on the PZT pulse waveform accompanied by ECG, pulse-oximetry, respiratory chart and accelerometer was developed as Figure 6 shows.

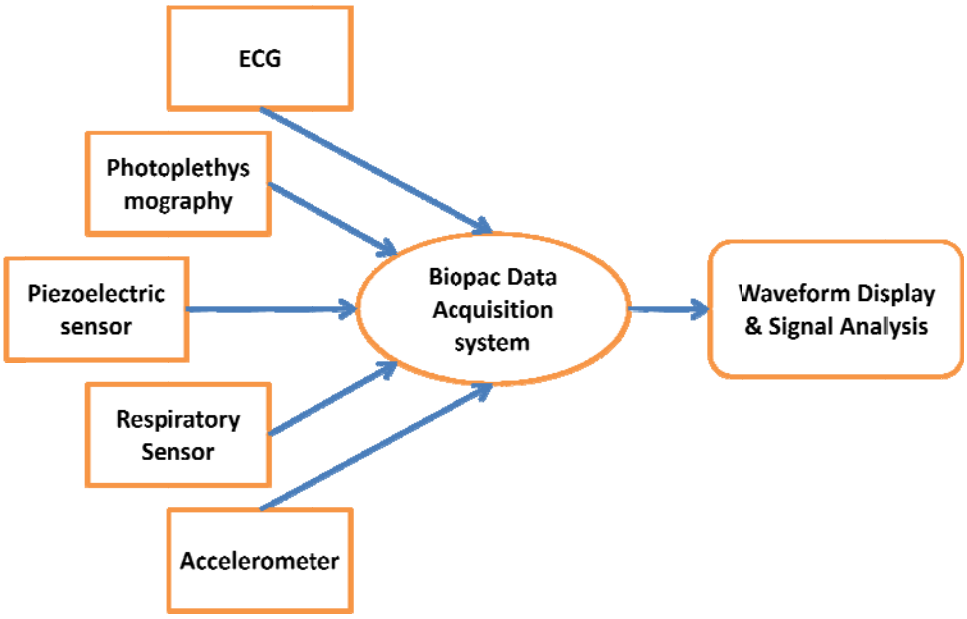

Figure 6, Monitoring System

2.3.1 Respiratory Flow Sensor

In 1908, Thomas Lewis studied the relationship between respiration and blood pressure [38]. Respiration affects blood volume as well as blood pressure in peripheral blood vessels. In one example, the Valsalva Maneuver can lead to dramatic blood pressure changes [39, 40]. During inhalation, the volume of the thoracic cavity increases which causes a relatively lower pressure in the lungs, so the peripheral blood is drawn into the lung vessels which creates a lower blood volume in the peripheral blood vessels. Contrarily, during exhalation, higher pressure in the lungs will force blood out into peripheral blood vessels which causes a higher blood volume. Studying the connection between respiration and pulse waveforms is helpful to understanding the cardiovascular system and to defining the features of PZT pulse waveform. Hence, a respiratory monitoring device is essential in our project.

A negative temperature coefficient (NTC) thermistor was placed under the nasal orifice to serve as a respiration sensor. A thermistor is a type of resistor

in which the resistance varies with temperature. The relationship between resistance and temperature in a NTC is indirectly proportional. In most cases, room temperature is below body temperature which is 37 degrees Celsius. During respiration, people inhale relatively cooler air and exhale relatively warmer air, this temperature change will be captured by the thermistor then translated to electrical signal to be recorded by Biopac system. The signal is a reflection of respiration conditions with no time delay.

A Wheatstone bridge circuit was used to convert the resistance change of the thermistor to voltage change which could be recorded by Biopac acquisition system. Figure 7 shows the circuit diagram of the Wheatstone bridge and amplifier. The bridge circuit was supplied by a 5 volts power supply. R1, R2 had the same resistance of 9.8 kohm. Rx was set to a value similar to the resistance of thermistor in normal room temperature. The output of the bridge was measured between points A and B which were then differentially with an AD-524 instrumentation amplifier with a gain of 10. Once there is a resistance change on the thermistor, a voltage difference occurs between point A and B. The signal was amplified and filtered then sent to the Biopac system to be displayed as a respiration waveform.

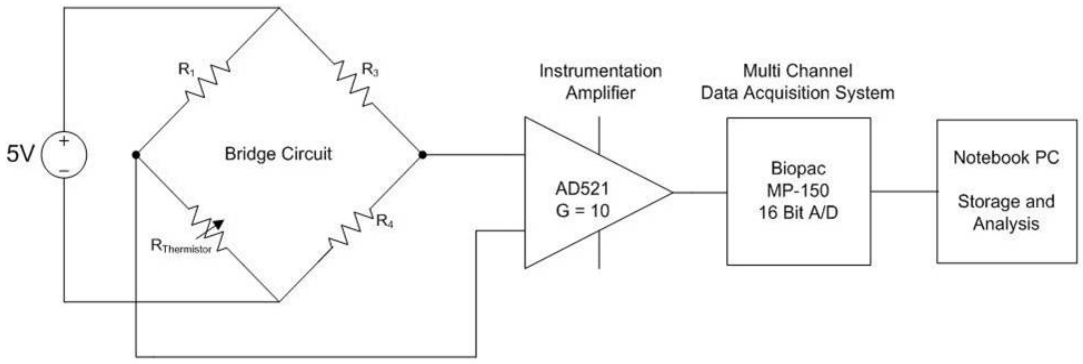

Figure 7, Bridge Circuit and Amplifier

Another method to monitor respiration taken into consideration was using a CO_2 sensor provided by Biopac System. The reason for using a thermistor instead of the CO_2 sensor was that the respiration waveform from the CO_2 sensor has a fair amount of time delay compared to the PZT pulse wave, pulse-oximetry and ECG signals which transmit form the body to the acquisition system in no time. This is because the CO_2 sensor is located in the Biopac base and connects to patient's mouth through a tube and it takes time for the airflow to travel the length of a tube that is one meter in length. The time delay would potentially cause problems in determining the relationship between respiration and pulse wave.

2.3.2 Accelerometer

An ADXL203 chip was used in the project (Analog Devices, Norwood, MA). It is a high precision, low power and dual-axis accelerometer with signal conditioned voltage outputs. It can measure acceleration with a full-scale range of ±1.7 g and it is sensitive to both dynamic and static acceleration [41]. In this experiment it was used to detect small finger movements which may or may not be shown in the PZT waveform. The ADXL203 has provisions for band limiting the X_{OUT} and Y_{OUT} pins. Capacitors must be added at these pins to implement low-pass filtering for anti-aliasing and noise reduction [41]. The equation for 3 dB bandwidth is

$$F_{-3\ dB} = 1/(2\pi(32\ k\Omega) \times C_{(X,\ Y)})$$

Or more simply,

$$F_{-3\ dB} = 5\ \mu F/C_{(X,\ Y)}$$

Since the movement of the body appeared to be low, two 0.47 µF capacitors

were used to limit the bandwidth of the accelerometers to less than 10 Hz. A 5 volt power supply was connected to the chip to run the internal amplifier and the X_{OUT} and Y_{OUT} pins were connected to Biopac system as shown in Figure 8.

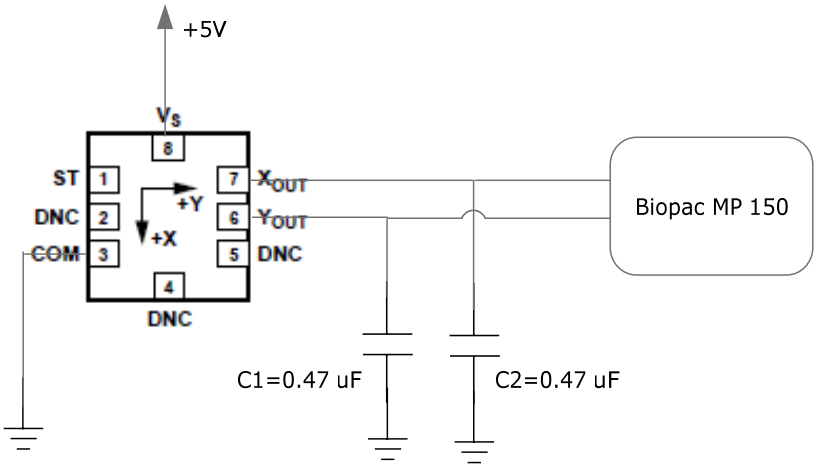

Figure 8, Circuit Diagram of ADXL203

The accelerometer was taped on the tip of the same finger to which the PZT sensor was attached. Since PZT was placed around the base segment of the finger, the movement that affected the pulse wave the most was bending the finger. When bending the favor, the tip of the finger moved the most which gave accelerometer strongest stimulation. The great sensitivity of accelerometer could ensure the recognition of any noise in the PZT pulse waveform which is cause by the movement of the finger.

CHAPTER 3

Methods

3.1 Testing Spots

Piezoelectric sensors detect mechanical change of peripheral arteries during pulsation through skin and soft tissue of the desired location. Anatomy differences affect the PZT pulse waveform depending on where the sensor is located on the body. Initially, locations were compared and contrasted to determine which location produced the strongest and cleanest signal. There are many locations on the human body at which arteries are close enough to the skin to allow the pulsation to be detected with a piezoelectric sensor. Digital arteries alongside the proximal phalanges of the hand, radial arteries at the wrist, brachial arteries from the inside of elbow, superficial temporal arteries from the temple, and a location just in front of the tragus were the five chosen locations used to test the sensor.

Since the radial artery is commonly used to take pulse measurements, it would be an ideal location to place the sensor. After being amplified 10 times, the signal amplitude produced at the wrist is about 1.5 volts to 2.5 volts, depending on the individual. However, a large amount of pressure is needed to keep a signal. The radial artery is along the medial edge of the radius and easily drops below the tendons of the wrist by way of any applied pressure or

movement. Therefore it is a usual occurrence to lose the signal when changing the angle of wrist joint and it was nearly impossible to detect a viable pulse signal when bending the wrist toward the front side of forearm. This eliminated the possibility of the wrist being a location for long-term monitoring. The signal, however, was enhanced by manually pressing the sensor to the wrist and since the wrist is one of the locations exhibiting the strongest pulsation in the human body, it may still be a good place to measure a short term pressure wave with the PZT sensor.

The Brachial artery on the inside of the elbow was the first spot to be completely eliminated. Observation showed that people with thinner arms could obtain a far better measurement on brachial arteries. This may be because more muscle mass and/or thicker layers of adipose tissue prevent the contact between arteries and the sensor.

The head has some benefits as test location for the PZT pulse measurement. First, the superficial temporal arteries come up to the head from the cheek to the temple, which contains less muscle and fat than other places on the body no matter the individual. Thus, when doctors cannot obtain a pulse in the arm of patients with obesity they nearly always go to their heads to obtain pulse wave information. Additionally, trauma patients being monitored on an ambulance or an ICU tend to move their heads far less than any other part of the body and this may eliminate a vast amount of noise created by movement of the sensor. A headband with padding on the site of temple was used to affix the head sensor. The signal obtained from the temple was clearer than the signal obtained from wrist and inner region of the elbow.

The signal from the site right in front of tragus is as clear as the one from temple. However, a headband with padding did not work well at this location. A headphone-like housing to hold the sensor may prove to be the best solution for this location. Unfortunately, finding the right place to position the sensor was not simple. If it were a simple task, it could be one of the best locations for measuring the PZT pulse wave.

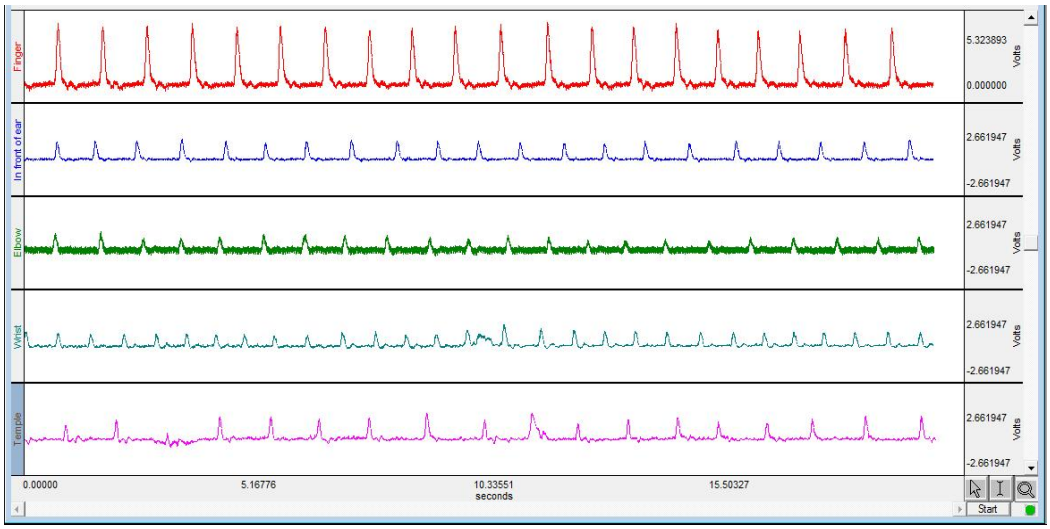

Figure 9, PZT Waveform from Different Spots

Form top: digital artery aside finger, superficial temporal artery in front of ear, brachial artery in side of elbow, radial artery at the wrist and temporal artery from temple.

The sensors used in the descriptions above were obtained from the commercial Dymedix Corporation adult snore sensors. The sensor pad was placed flat on the surface of the skin because it was determined that bending this sensor creates excessive noise. Figure 9 shows the comparison of the pulse waveforms captured from the different locations on the body in the same scale. The top waveform from the digital arteries aside finger is recorded using self-made finger wrap sensor. As seen in the figure, the signal obtained from the finger was significantly greater in amplitude when compared to the other four sites. Moreover, the signal from finger is more reliable and

easier to obtain in terms of ease of placement. It has a relatively strong immunity to noise caused by body movement except for movement of the tested finger. Thus the best locations for PZT pulse monitoring are the digital arties along the side of the proximal phalanges. Table 1 shows a summary of the advantages and disadvantages of the different testing locations.

Table 1, Comparison of Different Testing Locations

Location	Advantage	Disadvantage
Radial arteries at the wrist	Artery is easy to find Relatively high pulsation	Signal easily get lost when the wrist is moved
Brachial arteries from the inside of elbow	Largest pulsation point on some individuals	Artery is very hard to find on some individuals
Superficial temporal arteries from the temple	Relatively clear signal	Finding the right testing spot takes some time
Superficial temporal arteries in front of the tragus	Very clear signal	Special device to maintain the sensor contact is needed
Digital arteries alongside the proximal phalanges	Clearest and most reliable signal Placing the sensor is very easy	Sensor must be created manually

3.2 Experiential Procedure

3.2.1 Comparison of PZT and PPG waveform

PZT sensors do not record the real value of blood pressure; instead it records the change in pressure. The first step to understand the PZT pulse wave is comparing it to an existing, fully-understood, pulse monitoring method. In this study, a finger pulse oximeter was used to record the PPG waveform at the tip

of the same finger on which the PZT sensor was wrapped. ECG was also recorded at the same time as a reference.

3.2.2 Testing the correlation between PZT waveform and respiration

Four volunteers were used to test the PZT sensor, pulse-oximeter and breathe. During the test, subjects performed normal breaths, long deep breaths, and practiced breathe holding in both the sitting and prone positions. To ensure that all locations have the same correlation, the PZT sensor was also placed on the wrist, elbow, and temple areas to record the PZT waveform along with respiration monitoring.

3.2.3 Testing on temporal artery with different head vertical positions

An interesting phenomenon during the study was that the height of the peaks in the PZT pulse waveform changed with the change of vertical distance between testing spot and the horizontal level of heart. Therefore, a test was created placing a sensor on the temple and the head was moved to different vertical positions relative to the horizontal position of the heart. By defining the position of the heart as zero, signals were recorded on each person with their temporal artery at positions of 15, 25 and 36 cm above the heart.

3.2.4 Valsalva maneuver

A Valsalva maneuver is performed by a forcible exhalation against a closed airway, usually done by closing one's mouth and pinching one's nose shut. It is used in medical examinations as a test of cardiac function and autonomic nervous control of the heart. Valsalva maneuvers can lead to a series of physiological responses, mostly in the heart and cardiovascular systems and can result in measurable changes in heart rate, blood pressure, and pulse wave contour. Observation of a change of the PZT pulse waveform during

Valsalva maneuver is helpful to define the features of it. Therefore a short term and long term Valsalva maneuver tests with the PZT, pulse-ox, and ECG monitoring was designed.

3.2.5 Long term monitoring with accelerometer

When monitoring pulse waves by way of PZT for long periods of time, body movement affecting the PZT pulse waveform is inevitable. To more clearly distinguish signal from artifact an accelerometer was introduced into the system to monitor movement of the finger and compared to the artery pulsation signal. Tested subjects were asked to casually sit with the PZT sensor and accelerometer attached to one finger for 10 minutes or longer. During the test, subjects were free to move their finger and/or arm. The PZT pulse waveform and finger acceleration chart were recorded for future analysis.

CHPATER 4

Results and Analysis

4.1 The Character of PZT Pulse Waveform

According to an article discussing the relationship between wideband external pulse (WEP) wave and intra-arterial pulse wave by Payne [41], the WEP wave resembled the first derivative of the intra-arterial pressure pulse wave. The WEP signal was recorded using a broad bandwidth piezoelectric sensor located over the brachial artery, under the distal edge of a sphygmomanometer cuff, which has the same features as the PZT pulse waveform since they are both recording the artery pulsation using a piezoelectric sensor.

Figure 10 shows a PZT pulse waveform recorded at the bottom segment of middle finger and pulse oximeter waveform at the tip of the same finger. As shown in Figure 10 a time gap between the peaks of the PZT sensor and pulse oximeter sensors exists. The peak in the PZT waveform appears about 0.14 seconds earlier than the peak in the pulse oximeter waveform in the same cardiac cycle, which indicates something about the nature of the two signals. Pulse oximetry is a non-invasive method of monitoring the oxygenation of a patient's hemoglobin which is a reflection of blood pressure. PZT pulse waveform, on the other hand monitors the change of blood

pressure rather than directly monitoring blood pressure. The major peak in the PZT waveform ending at the same time that the SpO2 wave reaches its highest point indicates that the PZT has similar properties as the first derivate of the SpO2 pulse wave. The primary, or largest, peak in PZT waveform is indicative of increasing blood pressure and the second and third peak reflect notches in SpO2 waveform.

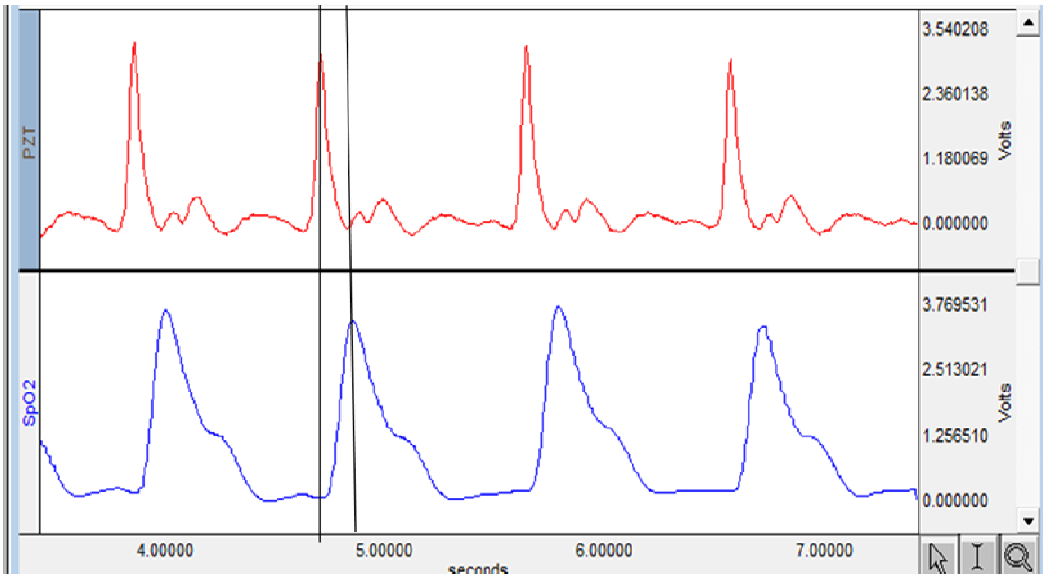

Figure 10, PZT and SpO2 Waveform

Top: PZT pulse waveform form bottom segment of middle finger; Bottom: SpO2 waveform form the tip of the same finger

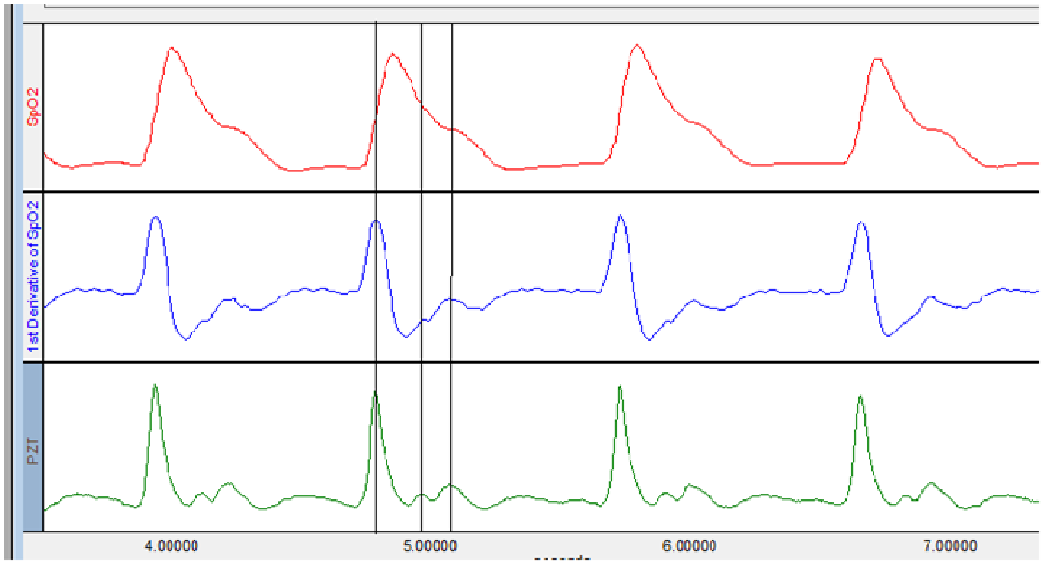

Figure 11, PZT and 1st Derivative of SpO2 Waveform

Top: SpO2 waveform; Middle: 1st derivative of SpO2 waveform; Bottom: PZT waveform with an experimental time shift of 0.08 seconds backward.

A comparison of a PZT pulse waveform and the 1st derivative of a SpO2 waveform is shown in Figure 11. From top to bottom are SpO2 waveform, 1st derivative of SpO2 and PZT pulse waveform with an experimentally added time shift, respectively. When 1st derivative of SpO2 waveform was compared to the PZT waveform, initially there was still a small mismatch of 0.08 seconds between the time peaks. The peaks in PZT waveform always appears about 0.08 seconds ahead of the peaks in the 1st derivative of SpO2 waveform. Therefore, this experimental time shift was added based on experimental results and analysis so that the peaks PZT pulse waveform and SpO2 waveform would properly align as shown in Figure 11.

The possibility that the time gap was exclusively caused by pulse wave propagation was eliminated during a test of pulse wave velocity by the use of two PZT sensors; one located on wrist and another on the finger tip. The results showed that pulse wave propagates from wrist to the end of finger in a

time less than 0.03 seconds. This means that the travel time of a pulse wave form the bottom segment of finger (PZT location) to the finger tip (SpO2 location) should be less than 0.015 seconds by a simple a distance ratio. Thus, the time shift in the peaks must be caused by the different type of pulse wave recording methods. It is acceptable that these two methods of measurement have a time difference as small as 0.08 seconds. Therefore, it was believed reasonable to add a time shift to either of the pulse waveforms to better analyze the correlation between the first derivative of SpO2 waveform and the PZT waveform.

As shown in Figure 11, SpO2 waves show a major peak, corresponding to the maximum blood pressure and a small deflection on the down stroke of waveform known as the dicrotic notch. The Dicrotic notch appears immediately following the closure of the semilunar valves and immediately preceding the dichotic wave, sometimes used as a marker for the end of systole or the ejection period. As mentioned in the introduction, peripheral pulse waveform usually has a much smaller inflection point between the main peak and the dicrotic notch as originally shown in Figure 3. In most cases, however, the SpO2 waveform fails to display this feature even though it can sometimes be observed in the 1st derivative of SpO2 waveform. The PZT pulse wave, on the other hand, shows three distinct peaks. Before the three peaks can be clearly defined, it is necessary to more precisely compare the PZT and SpO2 waveforms.

The contours of PZT waveform and 1st derivative of SpO2 are not quite the same, as observed showed in Figure 11. But after inclusion of a small time shift, it is observed that on the marked line in the time axis, the three peaks of

the PZT pulse wave almost perfectly match the peaks and inflection points in the 1st derivative of SpO2. The PZT wave form has the same characteristics as the 1st derivative of SpO2, which both represent the change of peripheral blood pressure wave. Therefore, the three peaks in PZT waveform represent the pulse peak, inflection point, and dicrotic notch respectively. The heights of the peaks in PZT correspond to the amount of change in blood pressure indicated, by the SpO2 waveform. A steeper curve in the SpO2 waveform resulted in a much larger (higher) peak in the PZT waveform. For instance, in most cases, larger pressure changes occur at that dicrotic notch rather than inflection point, as shown in Figure 11. As predicted, the corresponding peaks in PZT waveform show that the 3rd peak (dicrotic notch) is larger than the 2nd peak (inflection point). In another case as shown in Figure 12, pressure change in dicrotic notch can be too small to be easily recognizable or detected in the SpO2 waveform. The inflection point, however, is more easily observed. Fortunately, this situation is well expressed in the PZT waveform as the second peak is larger than the third but the third peak is still clearly visible.

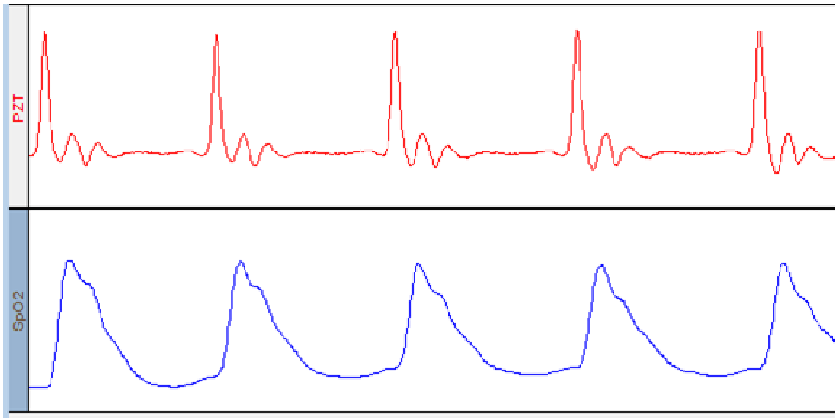

Figure 12, PZT and SpO2 without Dicrotic Notch

Dicrotic notch is smaller than inflection point. Top: PZT pulse waveform; Bottom: SpO2 waveform

Analyzing both Figure 11 and Figure 12, an advantage of PZT wave forms over SpO2 wave forms is that the PZT wave is more sensitive to smaller arterial pressure change and is able to capture the more important features of peripheral pulse wave, while SpO2 wave usually misses either the dicrotic notch or the inflection point. This alone makes PZT a more sensitive monitoring method compared to pulse oximetry.

Another advantage of PZT over SpO2 is that PZT monitoring provides more precise information when calculating the Heart rate variability (HRV). The time elapsing between two consecutive R waves (the largest peaks in an ECG measurement), more formally known as RR intervals, were extracted from ECG, PZT and SpO2 waveforms simultaneously. The Relative Mean Difference (RMD) of RR intervals between ECG and PZT was 0.51%, while the RMD between ECG and SpO2 was 0.77%.This seemingly small difference becomes significant, however, when comparing the calculated HRV. The RMD of HRV calculated from ECG and PZT was 11.73%, while the RMD of HRV calculated form ECG and SpO2 was 19.75%. Thus PZT monitoring provides approximately 8% greater accuracy when calculating HRV compared to extraction of HRV through pulse-oximetry.

4.2 PZT Pulse Wave and Respiration

Respiration is a major factor that affects the arterial blood pressure contour when people are in a state of rest. The pressure change in the thoracic cavity caused by the chest movement during respiration can lead to the peripheral blood being drawn into or pushed out of lung vessels. This can cause blood volume change in peripheral arteries and therefore change the blood pressure contour. The relationship between respiration and PZT pulse waveform was

examined and a method to derive respiration from the PZT pulse waveform signal was developed though signal processing.

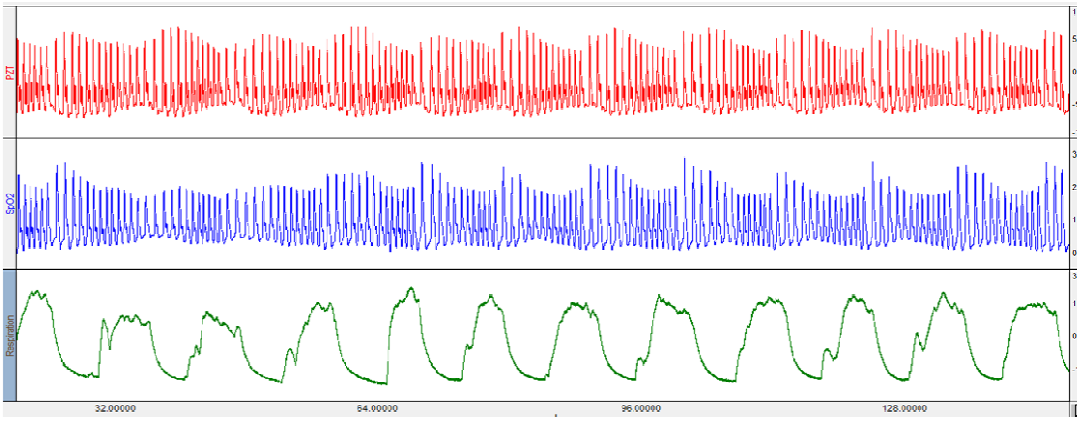

Figure 13, PZT, SpO2 and Respiration Waveform during Deep Breathing

Top: PZT pulse waveform; Middle: SpO2 waveform; Bottom: respiration waveform, during inhalation signal goes up, during exhalation signal goes down, the peaks show the maximum inhalation in each respiration cycle.

Figure 13 shows PZT and SpO2 pulse waveforms during three minutes of deep breathing. The bottom waveform is a respiration waveform recorded using a thermistor. During inhalation the signal level increases and during exhalation it decreases. Thus, in a single respiration cycle, the peak of the waveform represents the maximum inhalation and the start of exhalation, while the trough represents the stop of exhalation and the start of inhalation. As shown in Figure 13, the PZT waveform has a periodic contour change with respect to the respiration wave. During inhalation, the height of PZT pulse wave decreases gradually and during exhalation, the height of PZT pulse wave increases gradually. The maximum pulse peak during a respiration cycle always appears at the end of exhalation and in contrast, the minimum pulse peak occurs at the end of inhalation. The periodic contour change is so obvious in PZT waveform that respiration can be extracted even without using any processing tools. The contour of the SpO2 waveform, however, is not as

readily observable as the PZT signal although it does show periodicity according to respiration.

Figure 13 is not representative of normal breathing. Instead, the breath rate is as low as 6 breaths per minute as tested subjects were requested to take long deep breathes. This deep breathing method provides a much larger peripheral blood pressure change than normal breathing. The question remained, however, whether respiration could be derived from the PZT waveform in normal or even quick breathing patients. Unfortunately, in normal breathing the periodicity of the PZT waveform is not as easily observed as it is in slow, deep breathing. As a result, signal processing methods were used to find the hidden periodic character of the PZT waveform.

As shown in Figure 13, it is the amplitude of each pulse peak that makes the contour vary in an obvious respiration-like manor. Therefore, every major peak of the PZT pulse waveform must be analyzed to determine the correlation between this waveform and respiration. To accomplish this, a concept of pulse peak strength variation was introduced. This is defined as the amplitude variation of each pulse peak divided by the mean peak amplitude.

An algorithm written in MATLAB code (The MathWorks, Natick, MA) was used to extract pulse peaks from the PZT waveform. A 2^{nd} order lowpass digital Butterworth filter with cutoff frequency of 15 Hz was applied to reduce the high frequency noise including electrical noise at 60 Hz. A peak detection algorithm was then applied to the waveform. The detection algorithm used a threshold method to find the region where the main peak of every pulse cycle is located, including the maximum value within the region which is the pulse

peak. The threshold should be chosen carefully to avoid either missing one of the smaller pulse peaks or mistakenly counting one of the larger dicrotic notch peaks. An automatic threshold selecting method was used to handle most of the cases. This method can also be set manually to optimize the results. A similar method was used in detecting inhalation and exhalation in the respiration waveform.

The top and middle objects in Figure 14 show the result of pulse peak detection during a 60-second normal breathing test. The bottom figure shows the detection of the troughs of the respiration waveform which are the starting points of inhalation for each respiration cycle. The respiratory rate can be obtained directly by calculating the mean value of the intervals between inhalation starting points, which in this case is 16.77 breaths per minute. The pulse peak waveform shows fluctuation in a similar periodicity to the respiration waveform. A mathematic method to extract the periodicity of pulse peak wave was then performed to confirm the correlation between pulse peak wave and respiration.

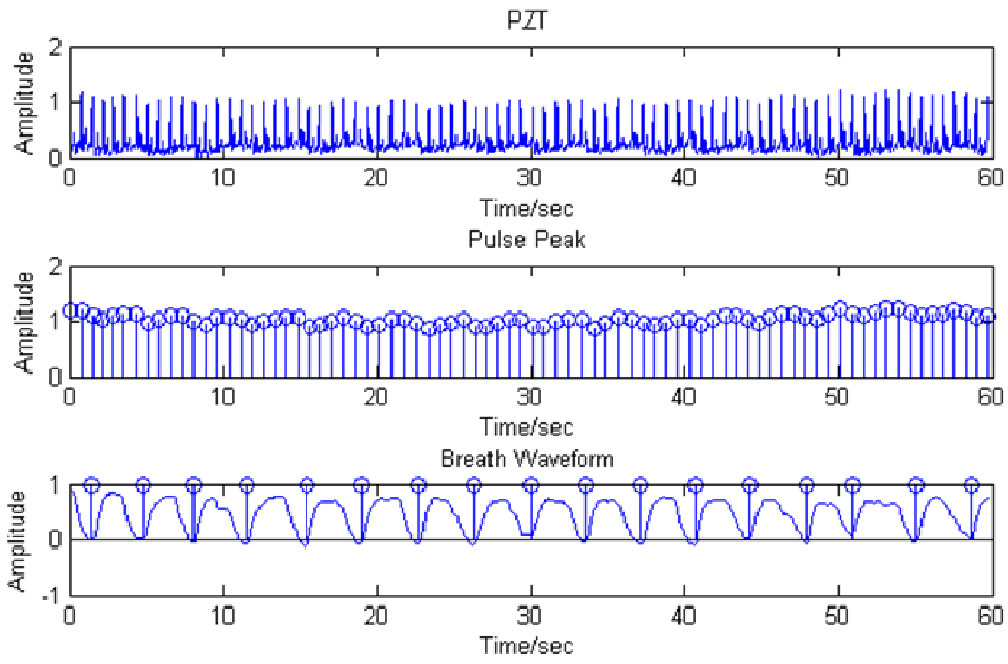

Figure 14, Peak Extraction from PZT and Respiratory Rate Detection

Figures based on 60 seconds normal breathing test. Top: PZT pulse waveform; Middle: pulse peak extraction from PZT waveform; Bottom: Detection of the start point of inhalation in respiration waveform

Computing the difference of each peak point from the mean gives us the pulse peak variation showed in the top and middle figures of Figure 15. Then using Fast Fourier Transform (FFT) the power spectrum of pulse peak variation was obtained as the bottom figure in Figure 15 shows. There are two major components in the frequency domain at 0.0167 Hz and 0.2845 Hz respectively. Comparing the pulse peak variation waveform in Figure 15 (middle), we can find the lower frequency at 0.0167 Hz is caused by baseline shifting of the sensor itself, and the periodic fluctuation associated with respiration is responsible for the higher frequency at 0.2845 Hz. Thus, an estimation of respiratory rate is 0.2845 Hz times 60 which compute to 17.07 breaths per minute. Comparing the actual respiratory rate of 16.77 breaths

per minute, to the estimated rate of 17.07 breaths per minute, corresponds to an error rate of less than 2%.

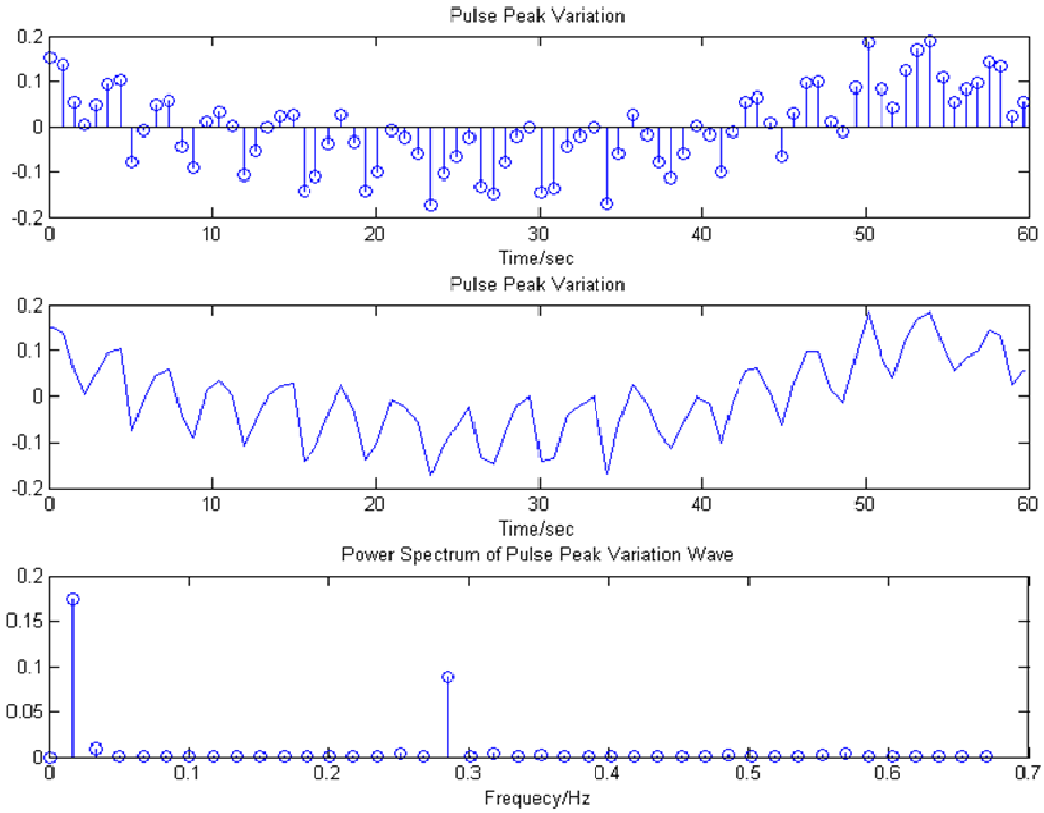

Figure 15, Pulse Peak Variation and it's Power Spectrum

A series of experiments were also performed to confirm that the connection between respiration and PZT pulse wave is not caused by the slight body movement through expansion of chest area during the respiration but indeed by the intrinsic relationship between the cardiovascular and respiratory systems. Sensor locations on the head, arm, wrist, and finger were all used in these tests and the results showed the same quality and the error between estimated respiratory rate and actual respiratory rate never exceeded 4%.

4.3 Pulse Strength at Different Head Positions

Systolic and diastolic peripheral blood pressure is most often measured in clinical practice with the arm at the same vertical level as the heart. If a patient raises his or her arm, the blood pressure when measured with a sphygmomanometer will change relative to the position of the heart. Considering that the heart is a pump, blood pressure when measured from the raising arm should be lower since the blood must be pumped to a higher level and more work must be done by the heart. When the arm is lowered below the level of the heart, blood pressure will increase and the heart does less work pumping blood to the arm. By convention, distances above the heart are considered positive while those below are considered negative. Given this convention, the blood pressure P given in Pascals for a given distance h above or below the position of the heart can be determined from Archimedes Principle,

$$P\ (Pascals) = P_0 - \rho g h \qquad (1)$$

where P_0 is the peripheral blood pressure at the heart level; ρ is the density of blood with an average value of 1.06 g/ml and g is the gravitational constant. The following relationship can be used to convert from Pascals to the more conventional measurement of blood pressure expressed in millimeters of mercury (mmHg). Given that the density of mercury is 13.6g/ml, the conversion formula from Pascals to mmHg is given by where the distance h is in millimeters

$$P(mmHg) = P_0 - 1.06 \cdot h/13.6 \qquad (2)$$

which simplifies to

$$= P_0 - 0.08 \cdot h \qquad (3)$$

The results of this work were similar to those obtained by Guss as shown in Table 2 [42] who determined the influence of arm position on blood pressure. The systolic and diastolic blood pressures are lower in arm position A (the arm is perpendicular to the torso) than in arm position B (the arm is parallel to the torso) because the vertical level of the sphygmomanometer is higher in position A as compared to position B.

Table 2, Blood Pressure Measurement in mmHg

Body	Arm	Systolic BP	Diastolic BP	Pulse Pressure
1	A	125.1	72.9	52.2
1	B	134.6	83.1	51.5
2	A	120.0	63.6	56.4
2	B	133.3	77.9	55.4

1 = standing; 2 = supine; A = arm perpendicular to the torso;
B = arm parallel to the torso

The response of the PZT pulse wave to peripheral blood pressure change for different vertical positions was also examined. A test was designed to measure blood pressure at the temporal artery with respect to several vertical positions of the head. The results in Figure 16 show that when the vertical position of head is higher than the heart level the PZT pulse wave has larger amplitude, even though previous studies show that the blood pressure should decrease when the head is at a higher level than the heart. This phenomenon means that PZT pulse amplitude increases when the blood pressure decreases and the amplitude decreases when the blood pressure rises. Although the reason for this phenomenon is not known, it can be used in predicting blood pressure change in the head caused by the Valsalva Maneuver or vertical acceleration of the body.

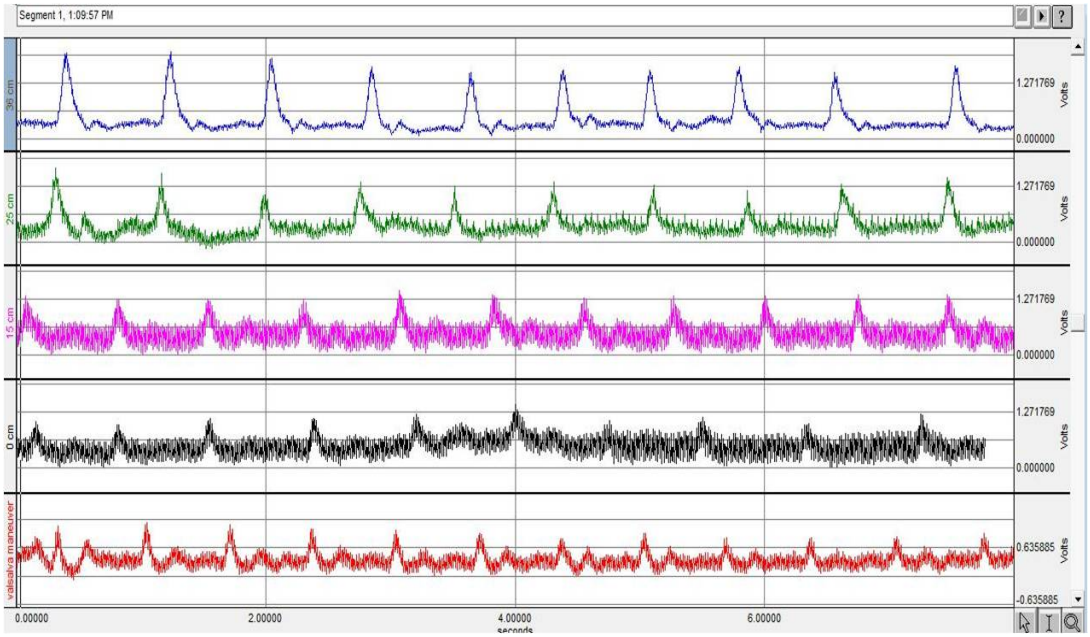

Figure 16, PZT Pulse Waveform in Different Head Positions

From top: (1): sitting up straight, vertical distance of temple over heart h is 36 cm; (2): h is 25 cm; (3) h is 15 cm; (4) supine, h is 0; (5) sitting straight up doing Valsalva maneuver

To measure the effect of head artery blood pressure change, a Valsalva maneuver was performed with the PZT sensor placed over the temporal artery, Figure 16 (5). With a test subject mean arterial blood pressure P_0 of 90 mmHg, the data were collected and pressure computed for four different head positions based on Equation 3 and summarized in Table 3.

Calculation of the blood pressure drop at the four head positions resulted in mean pressures of 62, 70, 78, 90 mmHg respectively. The mean pulse peak amplitude in PZT waveform was determined from the peak detecting algorithm. A PZT pulse peak amplitude chart corresponding to the mean pressure in head is shown in Figure 17. In this figure, the peak amplitude at 0.57 volts corresponds to a mean pressure of 83 mmHg. Thus, the estimated temporal artery pressure during the Valsalva maneuver reaches

approximately 83 mmHg which suggests that the maneuver results in a 21 mmHg increase in blood pressure measured by the PZT sensor at the location of the temporal artery.

Table 3, PZT Pulse Peak, Blood Pressure and Head Position

Head Position (cm)	Mean Pressure in Head (mmHg)	PZT Mean Peak Amplitude (volt)
36	62	1.27
25	70	0.88
15	78	0.67
0	90	0.43
Valsalva maneuver with head position at 36 cm	83 (Estimated)	0.57

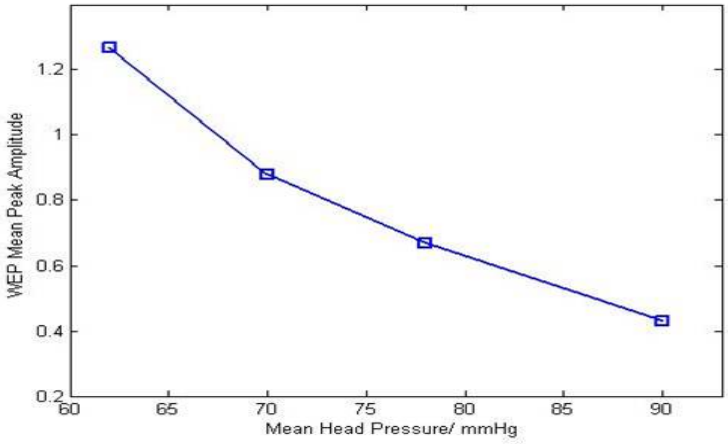

Figure 17, Mean Pressure in Head and PZT Pulse Peak Amplitude

X axis: Mean blood pressure in temporal arteries at temple; Y axis: Mean pulse peak amplitude in PZT waveform

4.4 PZT Waveform during Valsalva Maneuver

The Valsalva Maneuver (VM) is one of the most important autonomic tests and it provides specific information about vasomotor sympathetic functions [40]. Figure 18 shows the four phases of VM. A blood pressure increase occurs at the beginning of Phase I because a deep breath at the beginning of

VM increases the intrathoracic pressure. Early Phase II represents a decrease in blood pressure due to a reduced venous return to the heart. Approximately 10 seconds after breath holding, the increasing of noradrenergic-mediated peripheral resistance in turn increases systemic blood pressure in the late stages of Phase II. This is the most important part of the Valsalva maneuver since it provides a marker of peripheral resistance mediated by sympathetic vasomotor fibers [43].

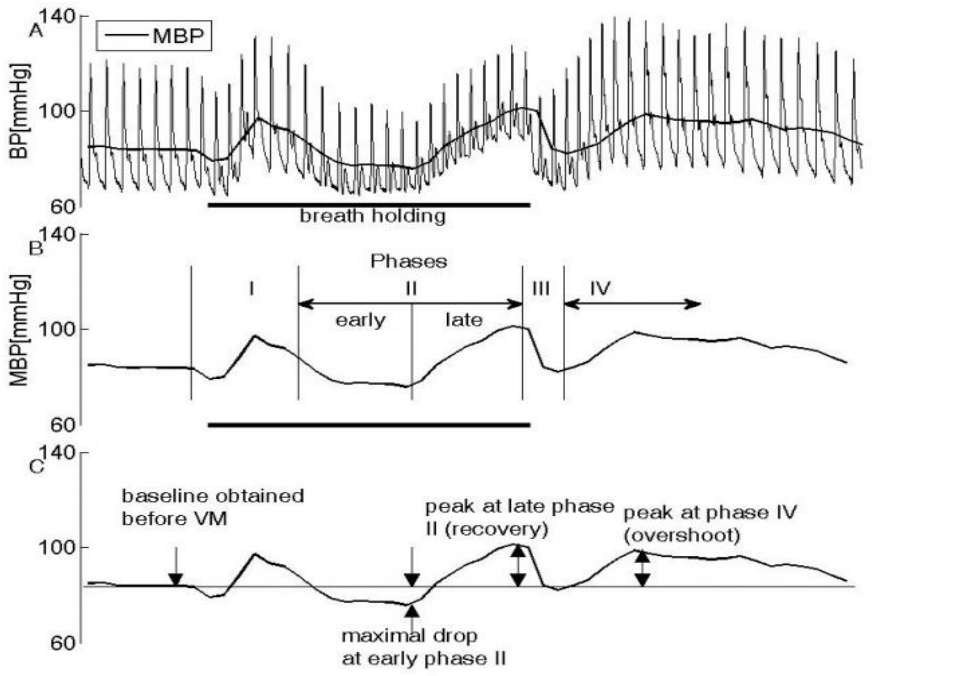

Figure 18, Intra-arterial Pressure Waveform during Valsalva Maneuver

Valsalva maneuver in a healthy subject (A) has four phases in blood pressure (B). Panel (C) shows how to correctly determine important variables from Valsalva maneuver including the maximal drop in the early Phase II, peak of the late Phase II (recovery) and overshoot during the Phase IV (C) [43].

Comparing PZT pulse waveform (Figure 19) in Valsalva maneuver to Figure 18, we can find occurrences of the different phases in the PZT pulse waveform. As showed in Figure 17, PZT pulse peak amplitude is reversely proportional to the mean blood pressure. At the beginning of the VM, pulse peak suddenly decreases represents the transiently increase of blood

pressure in Phase I. A gradual increase of the pulse peak amplitudes corresponds to the pressure drop which occurs at the early stage of Phase II; while the gradual decrease of the pulse peak amplitudes which starts at approximately ten seconds after the breath hold represents the pressure increase at the later stage of Phase II. Therefore PZT pulse waveform can be used to effectively test cardiac function and autonomic nervous control of the heart during Valsalva maneuver.

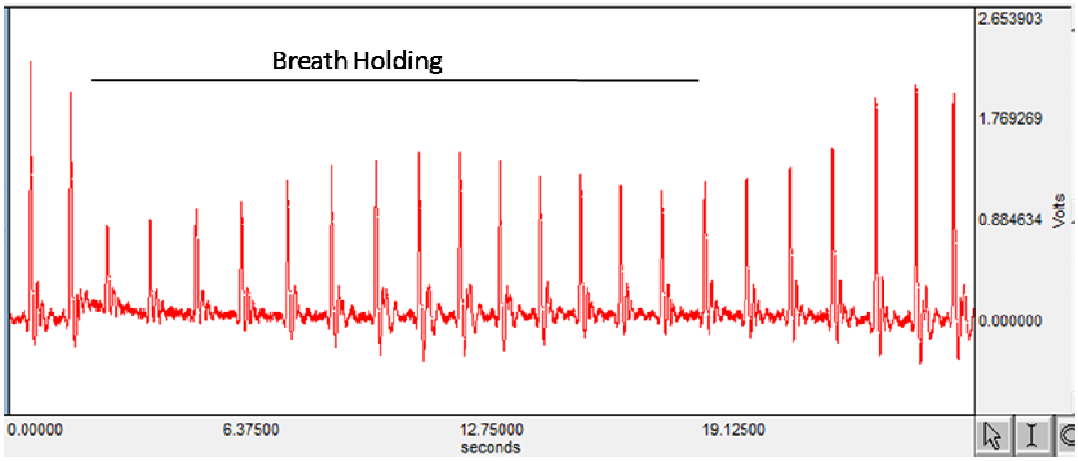

Figure 19, PZT Pulse Waveform in Valsalva Maneuver

CHAPTER 5

Conclusions and Future work

Using a piezoelectric sensor to monitor blood pressure is a fairly new concept given that it has only recently emerged in commercial practices. This may partially be attributed to the fact that it cannot generate the actual pressure waveform as intra-arterial pressure monitoring does. The use of PZT sensor based materials can provide a similar pressure contour as other actual pressure waveforms such as that of applanation tonometry and pulse-oximetry. The PZT pulse waveform, however, indicates the change of arterial pressure, which is similar to the 1st derivative of actual blood pressure waves. This work showed that the small inflections including the Inflection point and the Dicrotic notch in the intra-arterial pressure waveform are more precisely revealed on the PZT pulse waveform versus other methods.

As a non-invasive pulse monitoring system, applanation tonometry failed to give long term monitoring since most of the commercial devices provide a pen-shape tonometer that must to be pressed at the radial artery at the wrist. Any attempt to reform the tonometer to providing continuous monitoring was deemed inconvenient and complicated. In addition, the cost of a tonometry system can cost many thousands of dollars. Pulse-oximeter, on the other hand, is inexpensive and easy to use. Pulse oximetry cannot provide accurate

pressure information however, and often fails to accurately record and or detect the pulse waveform inflection points. PZT pulse wave monitoring compliments these two methods by providing a relatively sensitive and accurate measurement, using a low cost and convenient finger sensor wrap.

The high correlation between respiration waves and PZT pulse waves make PZT pulse monitoring a good method for indirectly monitoring not only the respiratory rate but also the quality of respiration. Therefore any hazard of apnoea or bradypnoea can be easily predicted by processing the PZT pulse waveform. The greater response to respiration also indicates that PZT pulse monitoring has a high sensitivity to blood volume change. This characteristic can be used to predict the severity of hemorrhage.

As a new type of arterial pressure recording, PZT pulse waveform is still not fully understood. Future studies on PZT pulse wave analysis may broaden the use of PZT pulse monitoring in its ability to predict and diagnose many other diseases associated with cardiovascular changes. Listed below are a few examples of future work to do for better manipulating and understanding the PZT pulse monitoring method.

(1) A pulse oximeter clip on the bottom section of finger with a PZT sensor surrounded inside could be made. The combination of PPG and PZT waveform will provide more detailed information about the peripheral blood pressure and volume.

(2) A headphone-like device with PZT sensor around the ear may provide a better result for monitoring temporal and posterior auricular arteries. Using the correlation between pulse peak strength and mean blood pressure, the head blood pressure change caused by body movement

and acceleration can be estimated. This way we can have a quantitative measurement of blood pressure change in studying the temporary blindness of pilot during aircraft acceleration or people's the head rush when standing up too fast.

(3) Simulating the PZT waveform of patient suffering from hemorrhage is highly relevant. The sensitivity to blood volume change may be used to predict the possibility and severity of hemorrhage. It could be used as a pre-indicator in ER for patients with the possibility of internal bleeding before sending them to a CT scan.

References

1. Alberto P Avolio et Arterial blood pressure measurement and pulse wave analysis- their role in enhancing cardiovascular assessment. Physiol. Meas. 2010, 31(1)
2. Fishman A P and Richards D W. Circulation of the Blood: Men and Ideas. 1964, (New York: Oxford University Press)
3. Noon JP. The Arterial Pulse Wave and Vascular Compliance. Prog. Cardiovasc. Nurs. 2009 Jun, 24(2): 53-8
4. Micheael F O'Rourke. Pulse wave analysis. Br J Clin Pharmacol. 2001,51(6): 507-522
5. Riva-Rocci S. Un nuovo sfigmomanometro Gazz. Med. di Torino 1896, 50: 981–1017
6. Korotkoff N S. A contribution to the problem of methods for the determination of blood pressure. Rep. Imp. Mil. Med. Acad. (St Petersburg) 1905,11: 365–7
7. http://en.wikipedia.org/wiki/Sphygmomanometer
8. Geddes L A. The Direct and Indirect Measurement of Blood Pressure.1970, (Chicago, IL: Year Book Medical Publishers)
9. O'Brien E and Fitzgerald D. The history of blood pressure measurement. J. Hum. Hypertens. 1994, 8: 73–84
10. Pressman G L and Newgard PM. A transducer for the continuous external measurement of arterial blood pressure. IEEE Trans. Biomed. Eng. 1963, 10: 73–81
11. Pressman G L and Newgard P M. Development of a blood-pressure transducer for the temporal artery. NASA Contract Report 1965, NASA CR-293 pp 1–63
12. Drzewiecki G M, Melbin J and Noordergraaf A. Arterial tonometry: review and analysis J. Biomech. 1983, 16: 141–52
13. Matthys K and Verdonck P. Development and modeling of arterial applanation tonometry: a review. Technol. Health Care 2002,10: 65–76
14. Sato T, NishinagaM, Kawamoto A, Ozawa T and Takatsuji H. Accuracy of a continuous blood pressure monitor based on arterial tonometry. Hypertension 1993, 21: 866–74

15. Chan G S, Middleton P M, Celler B G, Wang L and Lovell N H. Automatic detection of left ventricular ejection time from a finger photoplethysmographic pulse oximetry waveform: comparison with Doppler aortic measurement. Physiol. Meas. 2007,28: 439–52
16. Alty S R, Angarita-Jaimes N, Millasseau S C and Chowienczyk P J. Predicting arterial stiffness from the digital volume pulse waveform. IEEE Trans. Biomed. Eng. 2007, 54: 2268–75
17. Allen J. Photoplethysmography and its application in clinical physiological measurement. Physiol. Meas. 2007, 28: R1–39
18. CA Clark, EM Harmon. Hemodynamic monitoring: Pulmonary artery catheters. Techniques and Procedures in Critical Care,1990: 218-231
19. Gorny, D. A. Arterial Blood Pressure Measurement Technique. AACN Clinical Issues In Critical Care Nursing, 1993 Feb, 4(1): 66-80
20. Milnor W R. Hemodynamics 2nd edition. 1989, (Baltimore, MD: Williams & Wilkins)
21. Westerhof B E, Guelen I, Westerhof N, Karemaker J M and Avolio A. Quantification of wave reflection in the human aorta from pressure alone: a proof of principle. Hypertension, 2006, 48: 595–601
22. Kelly R, Hayward C, Avolio A and O'Rourke M. Noninvasive determination of age-related changes in the human arterial pulse. Circulation, 1989, 80: 1652–9
23. McEniery C M, Yasmin, Hall I R, Qasem A, Wilkinson I B, Cockcroft J R and ACCT Investigators. Normal vascular aging: differential effects on wave reflection and aortic pulse wave velocity: the Anglo-Cardiff Collaborative Trial (ACCT). J. Am. Coll. Cardiol. 2005, 46: 1753–60
24. Snieder H, Hayward C S, Perks U, Kelly R P, Kelly P J and Spector T D. Heritability of central systolic pressure augmentation: a twin study. Hypertension, 2000, 35: 574–9
25. Kelly R and Fitchett D. Noninvasive determination of aortic input impedance and external left ventricular power output: a validation and repeatability study of a new technique. J. Am. Coll. Cardiol. 1992, 20: 952–63
26. Verbeke F, Segers P, Heireman S, Vanholder R, Verdonck P and Van Bortel L M. Noninvasive assessment of local pulse pressure: importance of brachial-to-radial pressure amplification. Hypertension, 2005, 46: 244–8
27. Kelly R, Hayward C, Ganis J, Daley J, Avolio A and O'Rourke M. Noninvasive registration of the arterial pressure pulse waveform using high-fidelity applanation tonometry. J. Vasc. Med. Biol. 1989, 1: 142–9

28. Kroeker E J and Wood E H. Comparison of simultaneously recorded central and peripheral arterial pressure pulses during rest, exercise and tilted position in man. Circ. Res. 1955, 3: 623–32
29. Avolio A P. Multi-branched model of the human arterial system. Med. Biol. Eng. Comput. 1980, 18: 709–18
30. Karamanoglu M, Gallagher D E, Avolio A P and O'Rourke M F. Functional origin of reflected pressure waves in a multibranched model of the human arterial system. Am. J. Physiol. 1994, 267: H1681–8
31. Taylor M G. The input impedance of an assembly of randomly branching elastic tubes Biophys. J. 1966, 6: 29–51
32. Westerhof N, Bosman F, Vries C J D and Noordergraaf A. Analog studies of the human systemic arterial tree. J. Biomech. 1969, 2: 121–43
33. Karamanoglu M, O'Rourke M F, Avolio A P and Kelly R P. An analysis of the relationship between central aortic and peripheral upper limb pressure waves in man. Eur. Heart J. 1993, 14: 160–7
34. Fetics B, Nevo E, Chen C-H and Kass D A. Parametric model derivation of transfer function for noninvasive estimation of aortic pressure by radial tonometry. IEEE Trans. Biomed. Eng. 1999,46: 698–706
35. Hope S A, Meredith I T, Tay D and Cameron J D. 'Generalizability' of a radial-aortic transfer function for the derivation of central aortic waveform parameters. J. Hypertens. 2007,25: 1812–20
36. Tzou, H. S. and R. Ye. PYROELECTRIC AND THERMAL STRAIN EFFECTS OF PIEZOELECTRIC (PVDF AND PZT) DEVICES." Mechanical Systems and Signal Processing,1996, 10(4): 459-469.
37. http://en.wikipedia.org/wiki/Pvdf
38. Thomas Lewis Studies of the relationship between respiration and blood pressure. J Physil. 1908 ,37(3); 233-255
39. Walter E. Judson. Blood Pressure Responses to Valsalva Maneuver in Cardiac Patients with and without congestive Failure. Circulation, 1955,11:889
40. Fritsch-Yelle JM, Convertino VA, Schlegel TT. Acute manipulations of plasma volume alter arterial pressure responses during Valsalva maneuvers. J Appl Physiol. 1999, 86: 1852-1857
41. Payne RA, Isnardi D, Andrews PJ, Maxwell SR, Webb DJ. Similarity between the suprasystolic wideband external pulse wave and the first derivative of the intra-arterial pulse wave. Br J Anaesth. 2007 Nov, 99(5):653-61

42. Guss DA, Abdelnur D, Hemingway TJ. The impact of arm position on the measurement of orthostatic blood pressure. J Emerg Med. 2008 May, 34(4): 377-82.
43. http://autonomictesting.com/index.php?p=1_2_Valsalva-maneuver

Appendix

Matlab Codes for PZT Pulse Peak Detection, Respiratory waveform Analysis and Respiratory Rate Estimation

1. Pulse Peak Detection

```
clear all;
load data.mat,X;
fs=200;
X1=X(:,1);X2=X(:,3);
L=length(X1);


%---low pass filter
s=X1;
n=2; wn=15/(fs/2);
[b,a]=butter(n,wn,'low');
S0(1)=b(1)*s(1);
S0(2)=b(1)*s(2)+b(2)*s(1)-a(2)*S0(1);
for i=3:L
    S0(i)=b(1)*s(i)+b(2)*s(i-1)+b(3)*s(i-2)-a(2)*S0(i-1)-a(3)*S0(i-2);
end

SS=S0(51:L);
S0=SS;
L=L-50;

S0=S0+abs(min(S0));%............

Th=max(S0)*3/5;    %......may change for different signal 2/5 normal
j=0;
for i=1:L
    if S0(i)>Th
        j=j+1;
        QRS(j)=i;
    end
end

j=0;cnt=0;
for i=2:length(QRS)
    if QRS(i)-QRS(i-1)>fs/3
        j=j+1;
        count(j+1)=i-1-cnt;
        cnt=cnt+count(j+1);
        M=max(  S0 (   (QRS(i-count(j+1)):QRS(i-1))  )   );
        for k=(i-count(j+1)):(i-1)
            if S0(QRS(k))==M
            R(j)=QRS(k);
```

```
            end
        end
    end
end
M=max(  S0 (    QRS(cnt+1):QRS(i)   )   );
for k=(cnt+1):i
            if S0(QRS(k))==M
            R(j+1)=QRS(k);
            end
end


for i=1:length(R)
    P(i)=S0(R(i));
end

Xp=S0;
t=(1:length(Xp))/200;
figure,
subplot(3,1,1),plot(t,Xp),xlabel('Time/sec'),ylabel('Amplitude'),titl
e('PZT');
subplot(3,1,2),stem(R/200,P),xlabel('Time/sec'),ylabel('Amplitude'),t
itle('Pulse Peak');

%.........

AveragePulsePeak=mean(P);

SDPP=std(P);

RelativeStandardDeriation=SDPP/mean(P)

for i=1:(length(P)-1)
    Diff(i)=abs(P(i)-P(i+1));
end
%figure,plot(Diff,'.');

Differnce=sum(Diff)/i/mean(P)
```

2. Inhalation and exhalation extraction

```
%clear all
%load X_db,X;
fs=200;
X1=X(:,1);X2=X(:,3);
L=length(X2);

%---------------offset null

s=X2-mean(X2);
ss=s+max(s);
s=s/max(ss);
%s=-s;
%---------------low pass filter
n=2; wn=5/(fs/2);
[b,a]=butter(n,wn,'low');
S0(1)=b(1)*s(1);
S0(2)=b(1)*s(2)+b(2)*s(1)-a(2)*S0(1);
for i=3:L
    S0(i)=b(1)*s(i)+b(2)*s(i-1)+b(3)*s(i-2)-a(2)*S0(i-1)-a(3)*S0(i-2);
```

```
end

SS=S0(51:L);
S0=SS;
L=L-50-100; %.....................................
%------------------------------Peak Detection
S1=diff(S0);
j=0;k=0;
for i=6:L-6
    if and ((abs(S1(i))<0.001),S0(i)<0) %---0.0001 variables
derivation equals zero
        if and((S1(i-1)+S1(i-2)+S1(i-3)+S1(i-4)+S1(i-
5))<0,(S1(i+1)+S1(i+2)+S1(i+3)+S1(i+4)+S1(i+5))>0)
            if and(S0(i)<S0(i+50),S0(i+50)<S0(i+100))
                j=j+1;
                Insp0(j)=i;
            end
        end
    end
end

for i=length(Insp0):-1:2
    if abs(Insp0(i)-Insp0(i-1))<50    %-----100 variables
100/fs=0.5 second
        Insp0(i-1)=Insp0(i);
    end
end
j=0;
for i=1:(length(Insp0)-1)
    if Insp0(i)~=Insp0(i+1)
        j=j+1;
        Insp1(j)=Insp0(i);
    end
end

%------------
Insp1(j+1)=Insp0(length(Insp0));
j=0;
for i=2:length(Insp1)
    j=j+1;
    Tb(j)=Insp1(i)-Insp1(i-1);
end

%------------
j=0;
for i=1:length(Tb);
    j=j+1;
    if Tb(i)<mean(Tb)/3      %.........1/3 varibles
        j=j+1;
    end
    if (j-1)<=length(Tb)
        Insp2(i)=Insp1(j);
    end
end
if j<=length(Tb)
    Insp2(j+1)=Insp1(j+1);
end

Insp=Insp2;
Linsp=length(Insp);
```

```
subplot(3,1,3) ,
plot(t,(S0+abs(max(S0))));hold on,
stem(Insp2/200,ones(1,length(Insp2)));
xlabel('Time/sec'),ylabel('Amplitude'),title('Breath Waveform');

for i=1:Linsp-1
    T(i)=Insp(i+1)-Insp(i);
end

ResRate=60/mean(T)*fs
```

3. Respiratory rate estimation

```
[f,pf]=psp(P-mean(P),length(P)*fs/length(S0));

for i=2:length(f)
    if and (f(i)>0.12, f(i-1)<0.12)
        j=i;
    end
end
M=max(pf(j:length(f)));
for j=1:length(f)
    if pf(j)==M
        RespR=j;
    end
end

EstRate=f(RespR)*60
```

4. PSP Function

```
function [f,pF] = psp(s,fs)
t=length(s);
F=fft(s,t);
pF=F.*conj(F)/t;
f=fs*(0:t/2)/t;
```

Vita

Ruizhi Zhang was born on March 29th, 1984 in Qiqihar, Heilongjiang, China. He graduated from Shiyan High School in his hometown in 2003. He received his Bachelor of Science degree in Biomedical Engineering from Huazhong University of Science and Technology, Wuhan, Hubei, China in 2007. He is currently finishing his Master of Science degree in the same major from Virginia Commonwealth University.